

# **Recent Results from the BABAR Experiment<sup>\*</sup>**

BABAR Collaboration

Submitted to the International Conference On High-Energy Interactions:  
Theory And Experiment (Hadron Structure '02)  
22-27 Sep 2002, Herlany, Slovakia

*Stanford Linear Accelerator Center,  
Stanford University, Stanford, CA 94309*

---

<sup>\*</sup> Work supported by Department of Energy contract DE-AC03-76SF00515.

# Recent Results from the *BABAR* experiment

F. Salvatore<sup>1</sup>

Royal Holloway College, University of London, Egham, Surrey, TW20 0EX

(for the *BABAR* Collaboration)

We present an overview of some of the most recent results from the *BABAR* experiment. We discuss the latest measurement of the time-dependent *CP*-violating asymmetries in neutral *B* decays to several *CP* eigenstates, that in the Standard Model (SM) is proportional to  $\sin 2\beta$ . We present measurements of branching fractions and *CP*-violating asymmetries in neutral *B* decays to two-body final states of charged pions and kaons, that are related to the angle  $\alpha$  of the Unitarity Triangle. We also report the  $B^0$  lifetime measurement obtained from studying the  $B^0 \rightarrow D^{*-}\pi^+$  and  $B^0 \rightarrow D^{*-}\rho^+$  decay channels and the  $B^0 \rightarrow D^{*-}a_1^+$  branching fraction, obtained using a partial reconstruction technique. These measurements serve as a test and validation of the procedures required to measure the combination of CKM Unitarity Triangle angles  $\sin(2\beta + \gamma)$ .

## 1 Introduction

The study of *CP* violation has been a central concern of particle physics since it was discovered in 1964 [1]. In the Standard Model (SM), the *CP* violation in the weak interactions is a consequence of a complex phase in the three-generation Cabibbo-Kobayashi-Maskawa quark mixing matrix [2]. The unitarity of this matrix can be represented by the Unitarity Triangle in the complex plane, where the angles  $\alpha$ ,  $\beta$  and  $\gamma$  (also known as  $\phi_2$ ,  $\phi_1$  and  $\phi_3$ ) of the triangle are defined as follows:

$$\alpha = \arg\left(-\frac{V_{td}V_{tb}^*}{V_{ud}V_{ub}^*}\right), \quad \beta = \arg\left(-\frac{V_{cd}V_{cb}^*}{V_{td}V_{tb}^*}\right), \quad \gamma = \arg\left(-\frac{V_{ud}V_{ub}^*}{V_{cd}V_{cb}^*}\right). \quad (1)$$

As can be seen, these angles are related to parameters of the CKM matrix and the measurements of various *CP* asymmetries in *B* decays can be used to constrain their values.

In  $e^+e^-$  storage rings operating at the  $\Upsilon(4S)$  resonance, a  $B^0\bar{B}^0$  pair is produced in the  $\Upsilon(4S)$  decay and it evolves in a coherent *P*-wave state. If one particle is identified as a  $B^0$  at time  $t=0$ , it will oscillate between that state and the  $\bar{B}^0$  state with a frequency  $\Delta m_d$  determined by the mass difference of the two neutral *B* mass eigenstates. Because of Bose symmetry, the other *B* at the same time must be of opposite flavour. The time

---

<sup>1</sup>E-mail address: p.salvatore@rhul.ac.uk

distribution of  $B$  meson decays to a  $CP$  eigenstate (from now on referred as  $B_{rec}$ ), with the other  $B$  identified as a  $B^0$  or a  $\bar{B}^0$  ( $B_{tag}$ ), can be written in terms of a single complex parameter  $\lambda$  that depends on the  $B^0 - \bar{B}^0$  oscillation amplitude and the amplitudes describing  $B^0$  and  $\bar{B}^0$  decays to this final state. The decay rate  $f_+(f_-)$  when the  $B_{tag}$  is a  $B^0(\bar{B}^0)$  is given by:

$$f_{\pm}(\Delta t) = \frac{e^{-|\Delta t|/\tau_{B^0}}}{4\tau_{B^0}} [1 \pm S \sin(\Delta m_d \Delta t) \mp C \cos(\Delta m_d \Delta t)], \quad (2)$$

where  $S = \frac{2Im(\lambda)}{1+|\lambda|^2}$ ,  $C = \frac{1-|\lambda|^2}{1+|\lambda|^2}$ ,  $\Delta t = t_{rec} - t_{tag}$  is the time difference between the proper decay times of the two  $B$ 's and  $\tau_{B^0}$  is the  $B^0$  lifetime. The sine term in eq. 2 represents the interference between direct decay to the final state  $f$  and the decay after flavour oscillation, while the cosine term is due to interference between two or more decay amplitudes with different weak and strong phases that participate in the decay. It is possible to construct the following  $CP$  violating observable:

$$A_{CP}(\Delta t) = \frac{f_+(\Delta t) - f_-(\Delta t)}{f_+(\Delta t) + f_-(\Delta t)} = S \sin(\Delta m_d \Delta t) - C \cos(\Delta m_d \Delta t). \quad (3)$$

A non-zero value of this asymmetry between  $B^0$  and  $\bar{B}^0$  decay rates to the same  $CP$  final state is a proof of the existence of  $CP$  violation.

Observations of  $CP$  violation in  $B^0$  decays were already reported by *BABAR* [3, 4] and *Belle* [5, 6]; in this article we will review the most recent results from the *BABAR* experiment.

## 2 The *BABAR* Detector and Data Sets

The data used in the measurement we will describe in this paper were collected with the *BABAR* detector at the PEP-II storage ring from 1999 to 2002. These data correspond to an integrated luminosity of  $81 \text{ fb}^{-1}$  recorded at the  $\Upsilon(4S)$  resonance (the “on-resonance” sample) and about  $9 \text{ fb}^{-1}$  at a centre-of mass (CM) energy about 40 MeV below the  $\Upsilon(4S)$  resonance (“off-resonance”). The on-resonance sample contains about 88 million  $B\bar{B}$  pairs.

PEP-II is an asymmetric storage ring, with positron and electron beam energies of about 3.11 and 9.0 GeV. Therefore, the CM frame of the  $e^+e^-$  collision is boosted along the  $z$  direction in the laboratory frame, thus enabling time-dependent measurements of  $B$  mesons through vertex reconstruction. The average Lorentz boost is  $\langle \beta\gamma \rangle = 0.55$ . The *BABAR* detector is described in detail in ref. [7]; we give here a brief summary.

A silicon vertex tracker (SVT) made of 5 double-sided silicon layers surrounds the beam pipe and provides precise measurements of the trajectories of charged particles from the  $e^+e^-$  interaction point. A 40-layer drift chamber (DCH) surrounds the SVT and, together with it, provides measurements of track momenta and energy loss, which

contribute to the charged particle identification. A detector for internal Cherenkov Radiation (DIRC) is located outside the DCH and provides charged particle identification. Photon detection, electron identification and neutral hadrons reconstruction is provided by a CsI(Tl) electromagnetic calorimeter (EMC). All these detectors are inside a magnetic field of 1.5 T. Outside the coil of the superconducting magnet, the flux return yoke is instrumented with resistive plate chambers interspersed with iron (IFR) for the identification of muons and long-lived neutral hadrons.

### 3 The $\sin 2\beta$ measurement

In this section we will discuss the results obtained in the measurement of  $\sin 2\beta$  with the charmonium modes  $b \rightarrow c\bar{c}s$ , and the  $CP$  violating asymmetry of the Cabibbo-suppressed modes  $b \rightarrow c\bar{c}d$  and the pure penguin modes  $b \rightarrow s\bar{s}s$ .

#### 3.1 The “Golden Modes”: $b \rightarrow c\bar{c}s$

In the standard model, in case of charmonium-containing  $b \rightarrow c\bar{c}s$  decays, all the diagrams that contribute to the decay have the same weak phase. Therefore  $\lambda(b \rightarrow c\bar{c}s) = \eta_{CP} e^{-2i\beta}$ , where  $\eta_{CP}$  is the  $CP$  eigenvalue of the final state  $f$ . We reconstruct a sample of neutral  $B$  mesons decaying to the final states  $J/\Psi K_S^0$ ,  $\Psi(2S)K_S^0$ ,  $\chi_{c1}K_S^0$ ,  $\eta_c K_S^0$ ,  $J/\Psi K^{*0}(K^{*0} \rightarrow K_S^0 \pi^0)$  and  $J/\Psi K_L^0$ , and then examine each event for evidence that the recoiling  $B$  decayed as a  $B^0$  or a  $\bar{B}^0$ . The time-dependent  $CP$  asymmetry of eq. 3 in this case can be written as  $A_{CP}(\Delta t) = -\eta_{CP} \sin 2\beta \sin(\Delta m_d \Delta t)$ , where  $\eta_{CP} = -1$  for  $J/\Psi K_S^0$ ,  $\Psi(2S)K_S^0$ ,  $\chi_{c1}K_S^0$  and  $\eta_c K_S^0$ , and  $+1$  for  $J/\Psi K_L^0$ . Because of the presence of even ( $L=0, 2$ ) and odd ( $L=1$ ) angular momenta in the  $B \rightarrow J/\Psi K^{*0}$  decay, there can be contributions from  $CP$ -odd and  $CP$ -even amplitudes to the decay rate. Ignoring the angular information in the decay, the measured  $CP$  asymmetry in the  $J/\Psi K^{*0}$  final state is reduced by a dilution factor  $D_\perp = 1 - 2R_\perp$ , where  $R_\perp$  is the fraction of the  $L=1$  component. We have measured  $R_\perp = (16.0 \pm 3.5)\%$  [8], which gives  $\eta_{CP} = 0.65 \pm 0.07$  for this mode, after acceptance corrections.

The analysis procedure for all the analyzed modes, except  $\eta_c K_S^0$ , is described in detail in refs. [8, 9]. The  $B \rightarrow \eta_c K_S^0$  sample selection is described in ref. [10]. In brief, the  $J/\Psi$  and  $\Psi(2S)$  mesons are reconstructed through their decays to  $e^+e^-$  and  $\mu^+\mu^-$ ; the  $\Psi(2S)$  is also reconstructed through the  $J/\Psi \pi^+\pi^-$  decay mode. The  $\chi_{c1}$  meson is reconstructed in the  $J/\Psi \gamma$  decay mode, and the  $\eta_c$  meson in the  $K_S^0 K^+\pi^-$  and  $K^+K^-\pi^0$  modes<sup>1</sup>. Candidates in  $J/\Psi K_S^0$ ,  $\Psi(2S)K_S^0$ ,  $\chi_{c1}K_S^0$  and  $J/\Psi K^{*0}$  decay modes are selected requiring that the difference  $\Delta E$  between their energy and the beam energy in the centre-of-mass frame is less than three standard deviations from zero. In the  $J/\Psi K_L^0$  mode, the signal region is defined by  $|\Delta E| < 10$  MeV. The  $B \rightarrow \eta_c K_S^0$  candidates are required to have  $|\Delta E| < 40$  and 70 MeV for  $K_S^0 K^+\pi^-$

<sup>1</sup>Charge conjugation is always implied throughout the paper, unless otherwise stated.

and  $K^+K^-\pi^0$  modes respectively. For all modes except  $J/\Psi K_L^0$ , we define another kinematical variable, the beam substituted mass  $m_{ES} = \sqrt{(E_{beam}^{cm})^2 - (p_B^{cm})^2}$  and the signal region is defined by  $5.270(5.273) < m_{ES} < 5.290(5.288)$  GeV/c<sup>2</sup> for modes containing  $K_S^0$  ( $K^{*0}$ ).

To determine the flavour of the  $B_{tag}$  we use a multivariate algorithm based on neural networks. The tagging algorithm is fully described in ref. [3]. We select primary leptons from semi-leptonic  $B$  decays from identified muons, electrons and isolated energetic tracks. Kaon tags are defined by using the charge of the best kaon candidate in the event. Moreover, soft pions from  $D^{*-} \rightarrow \bar{D}^0 \pi^-$  decays are selected on the basis of their momentum and direction with respect to the thrust axis of  $B_{tag}$ . All this information is used as input to a neural network that takes into account all the correlations between the different sources of flavour information and provide an estimate of the probability for an incorrect tag assignment ( $w$ ) for each event. Using this probability and the outputs of the previously mentioned physics-based algorithms, each event is assigned to one of four hierarchical, mutually exclusive tagging categories: **Lepton**, **Kaon I**, **Kaon II**, **Inclusive** [3]. The figure of merit for tagging is the effective tagging efficiency  $Q = \sum_i \epsilon_i (1 - 2w_i)^2$ , where  $\epsilon_i$  is the tagging efficiency for category  $i$ . The value of  $Q$  for this tagging algorithm is  $(28.1 \pm 0.7)\%$ , a relative improvement of about 7% with respect to the tagging algorithm used in ref. [9].

The time interval  $\Delta t$  between the decay of the  $B_{rec}$  and  $B_{tag}$  is calculated from the measured separation  $\Delta z$  along the collision axis  $z$  of the two  $B$  vertices and the known boost of the  $e^+e^-$  system [9]. The  $z$  position of the  $B_{rec}$  vertex is determined from its charged tracks. The  $B_{tag}$  vertex is defined by fitting to a common vertex all the tracks that do not belong to the  $B_{rec}$  candidate, using constraints from the beam spot location and the  $B_{rec}$  momentum [9]. We select events with  $|\Delta t| < 20$  ps and  $\sigma_{\Delta t} < 2.5$  ps; 95% of the events satisfy these requirements. In Table 1 we list the number of events and the signal purity for the tagged  $B_{rec}$  sample [3]. The  $m_{ES}$  distribution for modes containing a  $K_S^0$  or  $K^{*0}$  and the  $\Delta E$  distribution for the  $J/\Psi K_L^0$  candidates are shown in Figure 1 (left). The measurement of  $A_{CP}$  requires the determination of the  $\Delta t$  resolution function and the fraction of mistag events  $w$ . These have been determined from real data using a sample of fully reconstructed  $B^0$  mesons that decay to flavour eigenstates ( $B_{flav}$ ) consisting of the channels  $D^{(*)-} h^+$  ( $h^+ = \pi^+, \rho^+, a_1^+$ ) and  $J/\Psi K^{*0} (K^{*0} \rightarrow K^+ \pi^-)$ .

We determine  $\sin 2\beta$  with a simultaneous unbinned maximum likelihood fit to the  $\Delta t$  distributions of the tagged  $B_{rec}$  and  $B_{flav}$  samples. The  $\Delta t$  distributions of the  $B_{rec}$  sample is described by eq. 2 with  $|\lambda| = 1$ . The  $\Delta t$  distribution for the  $B_{flav}$  sample evolve according to the known frequency for flavour oscillation in  $B^0$  mesons [3]. The observed amplitude for the  $CP$  asymmetry in the  $B_{rec}$  sample and for the flavour oscillation in the  $B_{flav}$  sample is reduced by the same amount  $(1 - 2w)$  due to flavour mistag. Events are assigned to the signal or background category based on the  $m_{ES}$  or  $\Delta E$  distributions. There are 34 free parameters in the fit: one for  $\sin 2\beta$ , 8 for the mistag fractions  $w_i$  and the difference  $\Delta w_i = w_i(B^0) - w_i(\bar{B}^0)$  between  $B^0$  and

Table 1 Number of events  $N_{tag}$  in the signal region after tagging and vertexing requirements, signal purity P and results of fitting for  $CP$  asymmetries in the  $B_{rec}$  sample (statistical error only).

Sample	$N_{tag}$	P(%)	$\sin 2\beta$
$J/\Psi K_S^0(\pi^+\pi^-)$	974	97	$0.82 \pm 0.08$
$J/\Psi K_S^0(\pi^0\pi^0)$	170	89	$0.39 \pm 0.24$
$\Psi(2S)K_S^0$	150	97	$0.69 \pm 0.24$
$\chi_{c1}K_S^0$	80	95	$1.01 \pm 0.40$
$\eta_c K_S^0$	132	73	$0.59 \pm 0.32$
Full $\eta_{CP} = -1$ sample	1506	94	$0.76 \pm 0.07$
$J/\Psi K_L^0$	988	55	$0.72 \pm 0.16$
$J/\Psi K^{*0}(K_S^0\pi^0)$	147	81	$0.22 \pm 0.52$
Full $CP$ sample	2641	78	$0.74 \pm 0.07$

$\bar{B}^0$  mistag fractions, 8 parameters for the signal  $\Delta t$  resolution. We also include 6 parameters for the background time dependence, 3 for its  $\Delta t$  resolution and 8 for the mistag fractions. We fix  $\tau_B = 1.542$  ps and  $\Delta m_d = 0.489$  ps<sup>-1</sup>[11] in the fit. The value of  $\sin 2\beta$  we obtain is[3]:

$$\sin 2\beta = 0.741 \pm 0.067 (stat) \pm 0.034 (syst). \quad (4)$$

Figure 1 (right) shows the  $\Delta t$  distributions and asymmetries in yields between  $B^0$  and  $\bar{B}^0$  tags for the  $\eta_{CP} = -1$  and  $+1$  samples, overlaid with the projection of the likelihood fit result. A number of consistency checks have been carried out on the  $B_{rec}$  sample. The results of the fit on the various sub-samples are shown in Table 1 and found to be statistically consistent.

We also measure the parameter  $|\lambda|$  from the  $\eta_{CP} = -1$  sample, which has the highest purity. We obtain  $|\lambda| = 0.948 \pm 0.051 (stat) \pm 0.030 (syst)$  and, in this case, the coefficient of the term  $\sin(\Delta m_d \Delta t)$  in eq.3 is  $0.759 \pm 0.074 (stat)$ .

This measurement of  $\sin 2\beta$  is consistent with the range implied by other experimental measurements and theoretical estimates of the magnitudes of the CKM matrix elements in the context of the SM.

### 3.2 The Cabibbo-suppressed $b \rightarrow c\bar{c}d$ modes

We report in this section the preliminary results on the  $CP$ -violating asymmetry of the Cabibbo-suppressed  $B^0 \rightarrow D^{*+}D^{*-}$ [12] and  $B^0 \rightarrow J/\Psi\pi^0$ [13] decay modes. In both this modes, the tree amplitude has the same weak phase as the  $b \rightarrow c\bar{c}s$  modes,

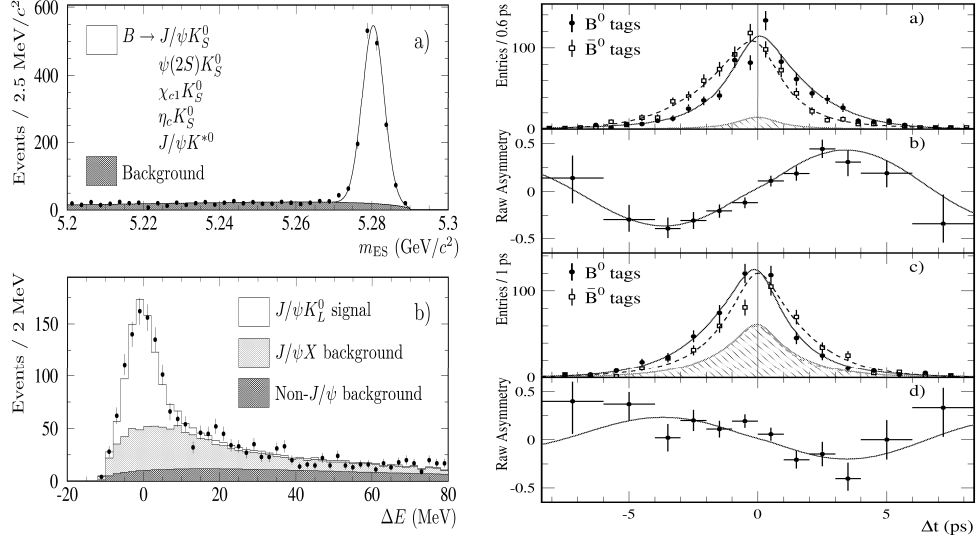


Fig. 1: Left: a)  $m_{ES}$  for final states containing a  $K_S^0$  or  $K^{*0}$ , and b)  $\Delta E$  for  $J/\Psi K_L^0$  candidates satisfying the tagging and vertexing requirements. Right: a) number of  $\eta_{CP} = -1$  candidates in the signal region with a  $B^0$  tag and a  $\bar{B}^0$  tag and b) raw asymmetry  $(N_{B^0} - N_{\bar{B}^0}) / (N_{B^0} + N_{\bar{B}^0})$  as a function of  $\Delta t$ . The solid (dashed) curves represent the fit projection in  $\Delta t$  for  $B^0$  ( $\bar{B}^0$ ) tags and the shaded regions represent the background contribution. The same is shown in c) and d) for the  $\eta_{CP} = +1$  mode.

but penguin-induced corrections are predicted, which can lead to a time-dependent  $CP$  asymmetry that differs from the one observed in  $b \rightarrow c\bar{c}s$  decays.

### 3.2.1 $B^0 \rightarrow D^{*+}D^{*-}$

In the framework of the SM, a  $CP$ -violating asymmetry related to  $\sin 2\beta$  is expected in the time evolution of the  $B^0 \rightarrow D^{*+}D^{*-}$  decays, as a result of the interference between direct  $B$  decay, expected to be dominated by the tree decay diagram, and decay after flavour change[14]. Penguin induced corrections of the order of 2% are expected in models based on the factorization approximation and heavy quark symmetry [15], therefore a comparison of measurements of  $\sin 2\beta$  from  $b \rightarrow c\bar{c}s$  modes with that obtained with this decay channel is an important test of these models and the consistency of the SM.

The analysis is fully described in ref. [12].  $B^0$  mesons are exclusively reconstructed by combining two charged  $D^*$  candidates reconstructed in a number of  $D^*$  and  $D$  decay modes. The primary variables used to distinguish signal from background are

also in this case  $m_{ES}$  and  $\Delta E$ . To measure the  $CP$  asymmetry, we use the same algorithms described in Section 3.1 to define the  $B_{rec}$  and  $B_{tag}$  vertices and the flavour of the tagging  $B$ , and also to determine the experimental  $\Delta t$  resolution function and the fraction of mis-tagged events  $w$ . The  $B^0 \rightarrow D^{*+}D^{*-}$  mode is a pseudo-scalar decay to a vector-vector final state, with  $CP$ -even ( $S$ - and  $D$ -waves) and  $CP$ -odd ( $P$ -wave) contributions. From the angular distribution of the  $B$  decay products we have measured that the  $CP$ -odd fraction  $R_{\perp}$  is  $0.07 \pm 0.06$  (*stat*)  $\pm 0.03$  (*syst*) [12]. The decay rate  $f_{\pm}$  for  $B^0$  mesons tagged as  $B^0(\bar{B}^0)$  of eq. 2 can be expressed in terms of the  $CP$ -even ( $\lambda_{+}$ ) and  $CP$ -odd ( $\lambda_{\perp}$ ) components of the complex  $CP$  parameter  $\lambda$  [12]. We determine the parameters  $Im(\lambda_{+})$  and  $|\lambda_{+}|$  with a simultaneous maximum likelihood fit to the  $\Delta t$  distributions of the  $B_{rec}$  and  $B_{flav}$  tagged samples. Because the  $CP$ -odd fraction is small, the parameters  $Im(\lambda_{\perp})$  and  $|\lambda_{\perp}|$  are poorly determined and therefore we fix them in the fit to -0.741 [3] and 1.0 respectively [12]. The preliminary results obtained from the fit are

$$\begin{aligned} Im(\lambda_{+}) &= 0.31 \pm 0.43 \text{ (stat)} \pm 0.13 \text{ (syst)}, \\ |\lambda_{+}| &= 0.98 \pm 0.25 \text{ (stat)} \pm 0.09 \text{ (syst)}. \end{aligned} \tag{5}$$

If the  $B^0 \rightarrow D^{*+}D^{*-}$  decay proceeds only through the  $b \rightarrow c\bar{c}d$  tree amplitude, we expect  $Im(\lambda_{+}) = -\sin 2\beta$ . To test this hypothesis, we fix  $Im(\lambda_{+}) = -0.741$  and repeat the fit. The observed change in the likelihood function corresponds to 2.7 standard deviations (statistical error only), therefore more data are needed to establish whether there are significant contributions from other processes, in particular penguin diagrams.

### 3.2.2 $B^0 \rightarrow J/\Psi\pi^0$

In the  $B^0 \rightarrow J/\Psi\pi^0$  decay there are two amplitudes that contribute: a portion of the penguin amplitude has the same weak phase as the tree amplitude, while the remainder of the penguin amplitude has a different phase [13]. In absence of those penguin contributions, the coefficients of the sine and cosine terms in eq. 3 would be  $S_{J/\Psi\pi^0} = -\sin 2\beta$  and  $C_{J/\Psi\pi^0} = 0$ . A statistically significant deviation from these values may indicate penguin contributions in  $B^0 \rightarrow J/\Psi\pi^0$  decays. The analysis procedure is fully described in ref. [13]. The methods for selecting the candidate events,  $B$  flavour tagging, vertex reconstruction and determination of the  $\Delta t$  resolution function are similar to those already described in the previous sections. We extract the  $CP$  asymmetry by performing an unbinned maximum likelihood fit. The resulting signal yield from  $81 \text{ fb}^{-1}$  is  $40 \pm 7$  events, and the results of the fit are  $S_{J/\Psi\pi^0} = 0.05 \pm 0.49$  (*stat*)  $\pm 0.16$  (*syst*) and  $C_{J/\Psi\pi^0} = 0.38 \pm 0.41$  (*stat*)  $\pm 0.09$  (*syst*). The error on the parameters is still statistically dominated, so more data need to be analyzed in order to establish  $CP$  violation in this channel.



## 4 The $\sin 2\alpha$ measurement

The time-dependent  $CP$ -violating asymmetry in the  $B^0 \rightarrow \pi^+\pi^-$  decay is related to the angle  $\alpha$  of the Unitarity Triangle. If the decay proceeds purely through the  $b \rightarrow u$  tree amplitude, the parameter  $\lambda$  of eq. 2 is given by

$$\lambda(B^0 \rightarrow \pi^+\pi^-) = \left(\frac{V_{tb}^* V_{td}}{V_{tb} V_{td}^*}\right) \left(\frac{V_{ud}^* V_{ub}}{V_{ud} V_{ub}^*}\right) \quad (6)$$

and the values of the coefficients of the sine and cosine terms in the asymmetry of eq. 3 are  $C_{\pi\pi} = 0$ ,  $S_{\pi\pi} = \sin 2\alpha$ . However, in general the  $b \rightarrow d$  penguin amplitudes participate in the decay and modify both the amplitude and the phase of  $\lambda$ . In this case, though, we have  $C_{\pi\pi} \neq 0$  and  $S_{\pi\pi} = \sqrt{1 - C_{\pi\pi}^2} \sin 2\alpha_{eff}$ , where  $\alpha_{eff}$  depends on the magnitudes and relative strong and weak phases of the tree and penguin amplitudes [4]. Several approaches have been proposed to obtain the value of  $\alpha$  from the measured  $\alpha_{eff}$  [16, 20].

### 4.1 The $B^0 \rightarrow h^+h'^-$ analysis

We reconstruct a sample of neutral  $B$  mesons decaying to the  $h^+h'^-$  final state, where  $h$  and  $h'$  are either a  $\pi$  or a  $K$ . We determine the signal yields with a maximum likelihood fit that includes kinematical, topological and particle identification information. For the  $B^0 \rightarrow K^-\pi^+$  decay, the yield is parametrized as  $N_{K^-\pi^+} = N_{K\pi}(1 \pm A_{K\pi})/2$ , where  $N_{K\pi}$  is the total yield and  $A_{K\pi} = (N_{K^-\pi^+} - N_{K^+\pi^-})/(N_{K^-\pi^+} + N_{K^+\pi^-})$  is the  $CP$ -violating charge asymmetry. This asymmetry is predicted to be less than 20% [16, 17] and is due to the interference between the  $b \rightarrow s$  penguin and  $b \rightarrow u$  tree amplitudes. Each event in the  $B_{rec}$  sample is examined to determine the flavour of the other  $B$  using the same tagging algorithm described in Section 3.1. The event selection,  $B_{rec}$  reconstruction and vertexing algorithms are also similar to those already described. Candidate  $B_{rec}$  decays are reconstructed from pairs of oppositely-charged tracks forming a good quality vertex. The pion mass is assumed for both tracks in calculating the four-momentum of the resulting  $B_{rec}$ . The identification of the  $h^+h'^-$  tracks as pions or Kaons is accomplished by measuring their Cherenkov angle  $\theta_c$  when traversing the DIRC. We construct double-Gaussian probability density functions (PDFs) from the difference between the measured and expected  $\theta_c$  for the pion and Kaon hypothesis, normalized by the error  $\sigma_{\theta_c}$ . The PDFs parameters are obtained from a sample of  $D^{*+} \rightarrow D^0\pi^+$ ,  $D^0 \rightarrow K^-\pi^+$  decays reconstructed in the data. The typical separation that is obtained between pions and Kaons varies from  $8\sigma_{\theta_c}$  at 2 GeV/c to  $2.5\sigma_{\theta_c}$  at 4 GeV/c. Signal decays are identified kinematically by requiring that  $5.20 < m_{ES} < 5.29$  GeV/c<sup>2</sup> and  $|\Delta E| < 0.15$  GeV [4]. Backgrounds from  $e^+e^- \rightarrow q\bar{q}$  ( $q = u, d, s, c$ ) processes are suppressed by their topology [4].

The time difference  $\Delta t$  between the  $B_{rec}$  and  $B_{tag}$  vertices and the  $\Delta t$  resolution function are obtained as already discussed in Section 3.1. We use an unbinned extended

maximum likelihood fit to extract the yields and  $CP$  parameters from the  $B_{rec}$  sample. The fitted sample contains 26070 events and the signal yields are determined excluding tagging or  $\Delta t$  information in the fit [4]. Table 2 summarizes the signal yields, the measured branching fractions and the charge asymmetry  $A_{K\pi}$ .

Table 2 Signal yields, charge-averaged branching fractions and charge asymmetry obtained in the  $B^0 \rightarrow h^+ h'^-$  analysis. Branching fractions are calculated assuming equal rates for  $\Upsilon(4S) \rightarrow B^0 \bar{B}^0$  and  $B^+ B^-$  decays. The upper limit for the  $B^0 \rightarrow K^+ K^-$  yield and branching fraction correspond to the 90% C.L.

Sample	$N_S$	$\mathcal{B}(10^{-6})$	$A_{K\pi}$	$A_{K\pi}$ 90% C.L.
$B^0 \rightarrow \pi^+ \pi^-$	$157 \pm 19 \pm 7$	$4.6 \pm 0.6 \pm 0.2$		
$B^0 \rightarrow K^+ \pi^-$	$389 \pm 30 \pm 17$	$17.9 \pm 0.9 \pm 0.7$	$-0.102 \pm 0.050$ $\pm 0.016$	$[-0.188, -0.016]$
$B^0 \rightarrow K^+ K^-$	$1 \pm 8 (< 16)$	$< 0.6$		

The parameters  $S_{\pi\pi}$  and  $C_{\pi\pi}$  are determined from a second fit that includes tagging and  $\Delta t$  information, where the  $B_{flav}$  sample is included to determine the signal parameters describing the tagging information and the  $\Delta t$  resolution function [4]. A total of 76 parameters are varied in the fit. We assume zero events from  $B^0 \rightarrow K^+ K^-$  decays and fix  $\tau_{B^0}$  and  $\Delta m_d$  to their world average values [11]. The combined fit to the  $B_{rec}$  and  $B_{flav}$  samples gives [4]:

$$\begin{aligned}
S_{\pi\pi} &= 0.02 \pm 0.34 (stat) \pm 0.05 (syst) \quad [-0.54, +0.58], \\
C_{\pi\pi} &= -0.30 \pm 0.25 (stat) \pm 0.04 (syst) \quad [-0.72, +0.12],
\end{aligned} \tag{7}$$

where the range in the brackets corresponds to the 90% C.L. interval, taking into account the systematic errors. Figure 2 shows the distributions of  $\Delta t$  for events with  $B_{tag}$  identified as  $B^0$  or  $\bar{B}^0$  and the asymmetry  $A_{\pi\pi} = (N_{B^0} - N_{\bar{B}^0}) / (N_{B^0} + N_{\bar{B}^0})$  as a function of  $\Delta t$ . We do not observe large mixing-induced or direct  $CP$  violation in the time-dependent asymmetry of  $B^0 \rightarrow \pi^+ \pi^-$  decays, as reported in [6].

## 4.2 The extraction of $\alpha$ from the measured $\alpha_{eff}$

As already discussed, the extraction of the angle  $\alpha$  from the  $B^0 \rightarrow \pi^+ \pi^-$  decays is complicated by the interference between  $b \rightarrow uW^-$  tree and  $b \rightarrow dg$  penguin amplitudes. Since these amplitudes have almost similar magnitudes but different weak phases, branching fraction measurements of the isospin-related decays  $B^\pm \rightarrow \pi^\pm \pi^0$  and  $B^0 \rightarrow \pi^0 \pi^0$  are needed in order to extract  $\alpha$  from the measured  $\alpha_{eff}$  [18]. Alternatively,

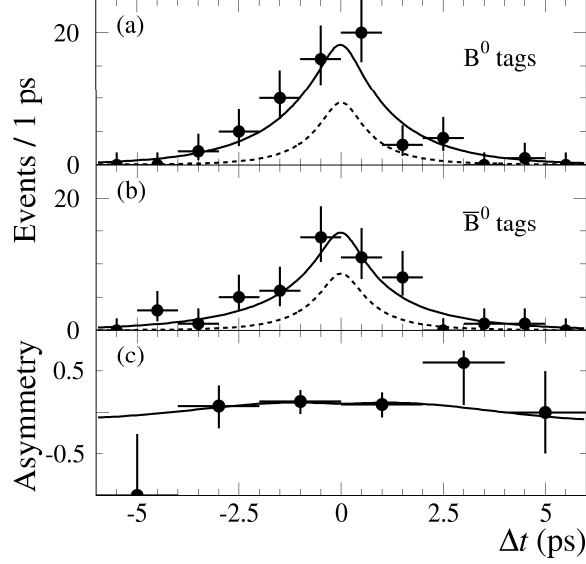


Fig. 2: Distributions of  $\Delta t$  for events enhanced in the signal  $\pi\pi$  decays with  $B_{tag}$  identified as a  $B^0$  (a) or  $\bar{B}^0$  (b); the plot (c) represents the asymmetry  $A_{\pi\pi}$  as a function of  $\Delta t$ . Solid curves represent projections of the maximum likelihood fit; dashed curves represent the sum of  $q\bar{q}$  and  $K\pi$  background events.

a bound on  $\alpha_{eff} - \alpha$  may be determined from the ratio  $\mathcal{B}(B^0 \rightarrow \pi^0\pi^0)/\mathcal{B}(B^+ \rightarrow \pi^\pm\pi^0)$ , using the average of the  $B^0$  and  $\bar{B}^0$  branching fractions [19].

#### 4.2.1 The $B^\pm \rightarrow h^\pm\pi^0$ branching fraction

The  $B^\pm \rightarrow \pi^\pm\pi^0$  decay is a pure tree decay to a very good approximation, and therefore no direct  $CP$  violation is expected. The event selection and  $B$  reconstruction of the  $B \rightarrow h\pi^0$  decay modes (where  $h = \pi^\pm, K^\pm$  and  $K^0$ ) is fully described in [21]. Hadronic events are selected based on track multiplicity and event topology. Charged  $\pi$  and  $K$  candidates are reconstructed within the fiducial volume of the detector, and  $\pi^0$  candidates are reconstructed from pair of photons with an invariant mass within  $3\sigma$  of the nominal  $\pi^0$  mass [11].  $K^0$  mesons are detected in the mode  $K^0 \rightarrow K_S^0 \rightarrow \pi^+\pi^-$ , and  $K_S^0$  candidates are selected from pairs of opposite charged tracks that form a good quality vertex and have an invariant mass within  $3\sigma$  of the nominal  $K_S^0$  mass [11]. Charged and neutral  $B$  candidates are then selected using the kinematical variables  $m_{ES}$  and  $\Delta E$ . The dominant background to these channels is composed of continuum  $e^+e^- \rightarrow q\bar{q}$  events and  $B$  decays into other light charmless final states ( $B^\pm \rightarrow \rho^\pm\pi^0$ ,

$B^0 \rightarrow \rho^\pm \pi^\mp$  and  $B^\pm \rightarrow K^{*\pm} \pi^0$ ) [21]. Continuum background is rejected by exploiting the different event topology between signal and background; the charmless background is instead reduced by applying a cut on  $\Delta E$  [21]. A total of 21752 candidates in the on-resonance data sample satisfy the  $B^\pm \rightarrow h^\pm \pi^0$  selection and 2668 satisfy the  $K_S^0 \pi^0$  selection. For each topology, we use an unbinned maximum likelihood fit to determine the signal and background yields  $n_i$  ( $i = 1, M$ , where  $M$  is the total number of signal and background types) and the  $CP$  asymmetry  $A_i = (\bar{n}_i - n_i)/(\bar{n}_i + n_i)$  [21]. The results of the fit are summarized in Table 3 (column 1 and 3), alongside the branching fractions computed for each channel. No evidence of direct  $CP$  asymmetry is observed.

Table 3 Signal yields, charge-averaged branching fractions and charge asymmetry obtained in the  $B^\pm \rightarrow h^\pm \pi^0$  analysis.

Sample	$N_S$	$\mathcal{B}(10^{-6})$	$A_i$	$A_i$ 90% C.L.
$B^\pm \rightarrow \pi^\pm \pi^0$	$125^{+23}_{-21} \pm 10$	$5.5^{+1.0}_{-0.9} \pm 0.6$	$-0.03^{+0.18}_{-0.17} \pm 0.02$	$[-0.32, 0.27]$
$B^\pm \rightarrow K^\pm \pi^0$	$239^{+21}_{-22} \pm 6$	$12.8^{+1.1}_{-1.2} \pm 1.0$	$-0.09 \pm 0.09 \pm 0.01$	$[-0.24, 0.06]$
$B^0 \rightarrow K^0 \pi^0$	$86 \pm 13 \pm 3$	$10.2 \pm 1.5 \pm 0.8$	$0.03 \pm 0.36 \pm 0.09$	$[-0.58, 0.64]$

#### 4.2.2 The $B^0 \rightarrow \pi^0 \pi^0$ branching fraction

The  $B^0 \rightarrow \pi^0 \pi^0$  analysis is fully described in [22].  $B^0$  candidates are formed from pairs of  $\pi^0$  candidates, each one formed from two neutral clusters with energy above 30 MeV and with an invariant mass within  $\pm 3\sigma$  of the nominal  $\pi^0$  mass [11]. Backgrounds from lepton pair and continuum  $q\bar{q}$  events are removed by exploiting the different event topology between signal (spherical topology) and background (two-jet like). The remaining background from  $q\bar{q}$  events with spherical topology and  $B^\pm \rightarrow \rho^\pm \pi^0$  decays in which the  $\pi^\pm$  is nearly at rest in the  $B$  frame are separated from signal by using the kinematical variables  $m_{ES}$  and  $\Delta E$  [22]. A total of 3020 candidates with  $m_{ES} > 5.2$  GeV/ $c^2$  and  $|\Delta E| < 0.2$  GeV are used in the analysis. The number of  $B^0 \rightarrow \pi^0 \pi^0$  events is determined from an unbinned maximum likelihood fit. The result of the fit is  $n_{\pi^0 \pi^0} = 23^{+10}_{-9}$  events [22], which corresponds to a branching fraction  $\mathcal{B}(B^0 \rightarrow \pi^0 \pi^0) < 3.6 \times 10^{-6}$  at 90% C.L. The central value of the likelihood fit is  $\mathcal{B}(B^0 \rightarrow \pi^0 \pi^0) = (1.6^{+0.7}_{-0.6} (stat)^{+0.6}_{-0.3} (syst)) \times 10^{-6}$ . The upper limit may be combined with our measurement of the  $B^\pm \rightarrow \pi^\pm \pi^0$  branching fraction to obtain a bound on the ratio  $\mathcal{R} = \mathcal{B}(B^0 \rightarrow \pi^0 \pi^0)/\mathcal{B}(B^\pm \rightarrow \pi^\pm \pi^0)$ . We find  $\mathcal{R} < 0.61$  at 90% C.L. and, assuming the isospin relations for  $B \rightarrow \pi\pi$  [19], this corresponds to an upper limit of  $|\alpha_{eff} - \alpha| < 51^\circ$  at 90% C.L.

## 5 Future goal: the $\sin(2\beta + \gamma)$ measurement

The neutral  $B$  meson decay modes  $B^0 \rightarrow D^{*-}h^+$ , where  $h^+$  is a light hadron ( $\pi, \rho, a_1$ ), have been proposed [23] for a theoretically clean measurement of the combination of CKM Unitarity Triangle angles  $\sin(2\beta + \gamma)$ . Since the expected time-dependent  $CP$  asymmetry in these modes is of the order of 2%, large data samples are needed in order to have a statistically significant measurement. For this reason, the technique of partial reconstruction of  $D^*$  mesons, in which only the soft pion ( $\pi_s$ ) from  $D^* \rightarrow D^0\pi$  decay is reconstructed, is used to select large samples of  $B$  mesons [24, 25, 26]. In this section, we will present some preliminary measurements of the  $B^0$  lifetime with partial reconstruction of  $B^0 \rightarrow D^{*-}\pi^+$  and  $B^0 \rightarrow D^{*-}\rho^+$  and the  $B^0 \rightarrow D^{*-}a_1^+$  branching fraction obtained using partially reconstructed events. These measurements constitute a first step toward measuring  $\sin(2\beta + \gamma)$  with this technique and these modes.

The analysis procedure for the three modes is fully described in [24], [25] and [26]. The data used in these analyses correspond to an integrated luminosity of  $20.7 \text{ fb}^{-1}$  on-resonance (22.7 million  $B\bar{B}$ ) and  $2.6 \text{ fb}^{-1}$  off-resonance. To partially reconstruct a  $B^0 \rightarrow D^{*-}h^+$  candidate, we compute the angle  $\theta_{Bh}$  between the  $B$  and  $h$  momentum vectors in the CM frame:  $\cos\theta_{Bh} = (M_{D^*}^2 - M_{B^0}^2 - M_h^2 + E_{CM}E_h)/2P_{B^0}|\vec{p}_h|$ , where  $M_x$  is the mass of particle  $x$ ,  $E_h$  and  $\vec{p}_h$  are the measured energy and momentum of the hadron  $h$  in the CM frame, and  $P_{B^0} = \sqrt{E_{CM}^2/4 - M_{B^0}^2}$ . Given  $\cos\theta_{Bh}$  and the four-momenta of  $h$  and  $\pi$ , the  $B$  four-momentum can be calculated up to an unknown azimuthal angle  $\phi$  around  $\vec{p}_h$ . For every value of  $\phi$ , the expected four-momentum of the  $D^0$  is determined and the  $\phi$ -dependent “missing mass”  $m(\phi)$  is calculated. We define the missing mass  $m(\phi) = \frac{1}{2}(m_{min} + m_{max})$ , where  $m_{min}$  and  $m_{max}$  are the minimum and maximum values of  $m(\phi)$  obtained by varying  $\phi$ . For signal events, this variable peaks around the nominal  $D^0$  mass [11], while background events are more broadly distributed. Event shape variables are used to suppress the continuum  $q\bar{q}$  background. In the  $B^0 \rightarrow D^{*-}\pi^+$  and  $B^0 \rightarrow D^{*-}\rho^+$  analyses, these variables are combined in a Fisher discriminant  $\mathcal{F}_D$  [24, 25], while in the  $B^0 \rightarrow D^{*-}a_1^+$  they are combined in a neural network  $\mathcal{N}$  [26]. In the  $B$  lifetime analyses, the decay position  $z_{rec}$  of the partially reconstructed  $B$  is determined by constraining the  $\pi_s$  and the  $\pi$  from  $B^0$  or  $\rho$  decay ( $\pi_h$ ) tracks to originate from the beam-spot in the  $x-y$  plane [24, 25]. The  $z_{other}$  position of the other  $B$  meson is obtained with all tracks excluding  $\pi_s$ ,  $\pi_h$  and any track whose CM angle with respect to the  $D^0$  direction is smaller than 1 radian. The decay time difference  $\Delta t$  between the two  $B$  mesons is then computed as already described in the previous sections. We require  $|\Delta t| < 15 \text{ ps}$  and  $\sigma_{\Delta t} < 2.4 \text{ ps}$  (4 ps for  $B^0 \rightarrow D^{*-}\rho^+$ ). The lifetime  $\tau_{B^0}$  is obtained from unbinned maximum likelihood fits with PDFs of  $\Delta t$ ,  $\sigma_{\Delta t}$  and  $m(\phi)$  [24, 25]. In the  $B^0 \rightarrow D^{*-}\rho^+$  analysis, the PDFs of  $\mathcal{F}_D$  and the  $\rho$  mass are also used. The results are  $\tau_{B^0} = 1.510 \pm 0.040 \text{ (stat)} \pm 0.038 \text{ (syst)}$  ps for  $B^0 \rightarrow D^{*-}\pi^+$  and  $\tau_{B^0} = 1.616 \pm 0.064 \text{ (stat)} \pm 0.075 \text{ (syst)}$  ps for  $B^0 \rightarrow D^{*-}\rho^+$ . The missing mass and  $\Delta t$  distribution of  $B^0 \rightarrow D^{*-}\pi^+$  and  $B^0 \rightarrow D^{*-}\rho^+$  events are

shown in Figure 3. The combined measurement, taking into account correlated errors, is  $\tau_{B^0} = 1.533 \pm 0.034$  (*stat*)  $\pm 0.038$  (*syst*) ps and is in good agreement with the world average  $B^0$  lifetime [11] and other *BABAR* results [8]. This establishes the validity of many of the techniques needed to measure  $\sin(2\beta + \gamma)$  using of partially reconstructed  $B^0 \rightarrow D^{*-}\pi^+$  and  $B^0 \rightarrow D^{*-}\rho^+$  events.

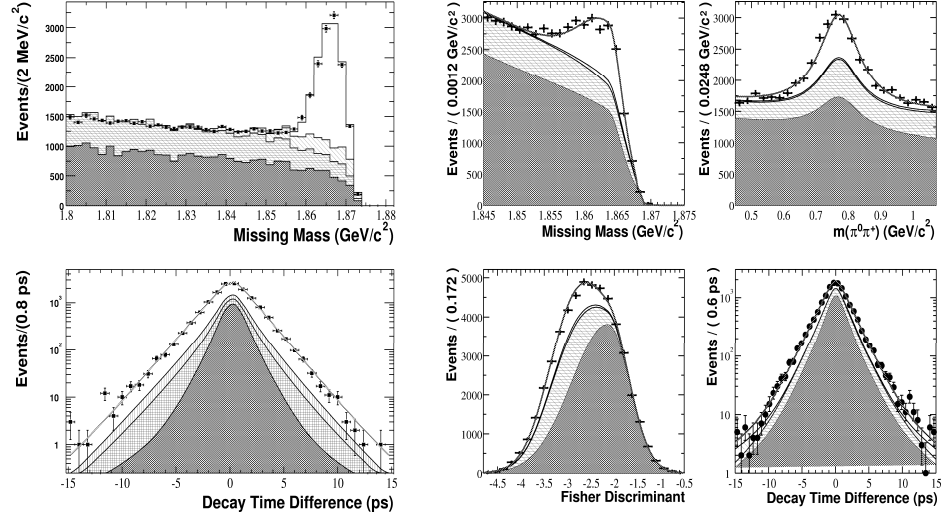


Fig. 3: Left: the missing mass (top) and  $\Delta t$  (bottom) distribution of  $B^0 \rightarrow D^{*+}\pi^-$  events. The  $\Delta t$  plot has been obtained after requiring  $m(\phi) > 1.860$   $\text{GeV}/c^2$ . Right: the missing mass,  $\rho$  mass, Fisher discriminant and  $\Delta t$  distribution of  $B^0 \rightarrow D^{*+}\rho^-$ . The  $\Delta t$  plot has been obtained after requiring  $m(\phi) > 1.854$   $\text{GeV}/c^2$ ,  $0.60 < m(\pi^+\pi^0) < 0.93$   $\text{GeV}/c^2$ , and  $\mathcal{F}_D < -2.1$ . In all plots, the result of the fit is superimposed on the data. The hatched, cross-hatched and shaded areas are the peaking  $B\bar{B}$ , combinatoric  $B\bar{B}$  and continuum background contributions, respectively.

In the  $B^0 \rightarrow D^{*-}a_1^+$  analysis, signal events are selected by requiring that the invariant mass of the  $3\pi$  state is between 1.0 and 1.6  $\text{GeV}/c^2$ , the invariant mass of at least one of the two possible  $\pi^+\pi^-$  combinations is in the range  $[0.278, 1.122]$   $\text{GeV}/c^2$ , and at least one additional track (the  $\pi_s$ ) with CM momentum between 50 and 700  $\text{MeV}/c^2$  is reconstructed [26]. The resulting  $m(\phi)$  distribution of on-resonance data, with off-resonance appropriately subtracted, is fitted using a minimum  $\chi^2$  technique to a linear combination of the  $m(\phi)$  distributions of  $B\bar{B}$  Monte Carlo (MC) events, excluding correctly reconstructed signal events, and correctly reconstructed signal MC events. In Figure 4 the  $m(\phi)$  distribution of on-resonance data, off-resonance subtracted, is shown, together

with the distributions of  $B\bar{B}$  MC and signal MC events. We obtain a signal yield of  $18400 \pm 1200$  events, corresponding to  $\mathcal{B}(B^0 \rightarrow D^{*-} a_1^+) = (1.20 \pm 0.07 (stat) \pm 0.14 (syst))$  %. This result is in good agreement with the current world average [11], but reduces the uncertainty by a factor of two.

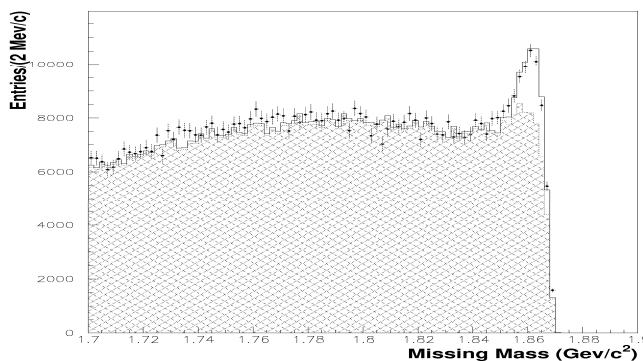


Fig. 4: Missing mass distribution of continuum-subtracted on-resonance data events (data points),  $B\bar{B}$  background MC events (hatched histogram) and  $B\bar{B}$  plus signal events (solid histogram) obtained in the  $B^0 \rightarrow D^{*-} a_1^+$  analysis.

## 6 Conclusion

We have reported some of the most recent results from the *BABAR* experiment. An improved measurement of the sine of the Unitarity Triangle angle  $\beta$  has been obtained with a data sample of about 88 million  $\Upsilon(4S) \rightarrow B\bar{B}$  decays:  $\sin 2\beta = 0.741 \pm 0.067 (stat) \pm 0.033 (syst)$ . This measurement is consistent with the Standard Model expectation. Preliminary results have been reported of the measurement of the  $CP$  asymmetry in the Cabibbo-suppressed modes  $b \rightarrow c\bar{c}d$  and  $b \rightarrow s\bar{s}s$ . In the framework of the SM, a  $CP$ -violating asymmetry related to  $\sin 2\beta$  is expected in both cases. The time-dependent  $CP$  asymmetry measurements still have large statistical uncertainties and these should be reduced in the coming years as *BABAR* accumulates data, allowing useful tests of the Standard Model.

We observe no evidence for large mixing-induced or direct  $CP$  violation in the time-dependent asymmetry of  $B^0 \rightarrow h^+ h'^-$  decays. The decay amplitude has contribution from both tree and penguin diagrams, therefore the measured  $CP$  asymmetry is proportional to the angle  $\alpha_{eff}$ . It is possible to extract the Unitarity Triangle angle  $\alpha$  from  $\alpha_{eff}$  by measuring the branching fraction of the isospin-related decays  $B^\pm \rightarrow \pi^\pm \pi^0$  and  $B^0 \rightarrow \pi^0 \pi^0$ . Preliminary measurements of these branching fractions has been reported

in this paper. A bound on the difference  $|\alpha_{eff} - \alpha|$  can be obtained from the ratio of branching fractions  $\mathcal{B}(B^0 \rightarrow \pi^0 \pi^0)/\mathcal{B}(B^\pm \rightarrow \pi^\pm \pi^0)$ . A preliminary result gives:  $|\alpha_{eff} - \alpha| < 51^\circ$  at 90% C.L.

We have reported the measurement of the  $B^0$  lifetime obtained with partially reconstructed  $B \rightarrow D^{*-} \pi^+$  and  $B \rightarrow D^{*-} \rho^+$ , and the measurement of  $\mathcal{B}(B \rightarrow D^{*-} a_1^+)$  with partial reconstructed events. The results are in good agreement with the corresponding world average values, establishing the validity of the use of partially reconstructed events in the measurement of  $\sin(2\beta + \gamma)$ .

### References

- [1] J.H.Christenson *et al.*: *Phys. Rev. Lett.* **13** (1964) 138; G.D.Barr *et al.*: *Phys. Lett.* **317** (1993) 233; K.L.Gibbons *et al.*: *Phys. Rev. Lett.* **70** (1993) 1203;
- [2] N.Cabibbo: *Phys. Rev. Lett.* **10** (1963) 531; M.Kobayashi, T.Maskawa: *Prog. Th. Phys.* **49** (1973) 652;
- [3] B.Aubert *et al.*: *Phys. Rev. Lett* **89** (2002) 20;
- [4] B.Aubert *et al.*: *hep-ex/0207055* (2002) (Submitted to *Phys. Rev. Lett*);
- [5] K.Abe *et al.*: *Phys. Rev.* **D66** (2002) 032007;
- [6] K.Abe *et al.*: *Phys. Rev. Lett.* **89** (2002) 071801;
- [7] B.Aubert *et al.*: *Nucl. Instr. and Methods* **A479** (2002) 1;
- [8] B.Aubert *et al.*: *Phys. Rev. Lett.* **87** (2001) 151802;
- [9] B.Aubert *et al.*: *Phys. Rev.* **D65** (2002) 051502;
- [10] B.Aubert *et al.*: *hep-ex/0203040* (2002) ;
- [11] Particle Data Group, K.Hagiwara *et al.*: *Phys. Rev.* **D66** (2002) 010001;
- [12] B.Aubert *et al.*: *hep-ex/0207072* (2002) ;
- [13] B.Aubert *et al.*: *hep-ex/0207058* (2002) ;
- [14] R.Aleksan *et al.*: *Phys. Lett.* **B317** (1993) 173;
- [15] X.Y.Pharm and Z.Z. Xing: *Phys. Rev.* **D458** (1999) 375;
- [16] M.Beneke, G.Buchalla, M.Neubert and C.T.Sachrajda: *Nucl. Phys.* **B606** (2001) 245;
- [17] A.Ali, G.Kramer and C.Lü: *Phys. Rev.* **D59** (1999) 0140054; Y.Y.Keum, H-n. Li and A.I. Sanda: *Phys. Rev.* **D63** (2001) 054008; M.Ciuchini *et al.*: *Phys. Lett.* **B515** (2001) 33;
- [18] M.Gronau and D.London: *Phys. Rev. Lett.* **65** (1990) 3381;
- [19] Y.Grossman and H.R.Quinn: *Phys. Rev.* **D58** (1998) 017504;
- [20] J.Charles: *Phys. Rev.* **D59** (1999) 054007; M.Gronau, D.London, N.Sinha and R.Sinha: *Phys. Lett.* **B514** (2001) 315;
- [21] B.Aubert *et al.*: *hep-ex/0207065* (2002) ;
- [22] B.Aubert *et al.*: *hep-ex/0207063* (2002) ;
- [23] P.F.Harrison and H.Quinn (ed.): *BABAR Physics Book*, Chap. 7.6, 1998; I.Dunietz and R.G.Sachs: *Phys. Rev.* **D37** (1988) 3186; I.Dunietz: *Phys. Lett.* **B427** (1998) 179;
- [24] B.Aubert *et al.*: *hep-ex/0207038* (2002) ;
- [25] B.Aubert *et al.*: *hep-ex/0207036* (2002) ;
- [26] B.Aubert *et al.*: *hep-ex/0207085* (2002) ;